LRRK2 phosphorylation of auxilin mediates synaptic defects in dopaminergic neurons from patients with Parkinson's disease

Maria Nguyen[a] and Dimitri Krainc[a,1]

[a]Ken & Ruth Davee Department of Neurology, Northwestern University Feinberg School of Medicine, Chicago, IL 60611

Recently identified Parkinson's disease (PD) genes involved in synaptic vesicle endocytosis, such as DNAJC6 (auxilin), have further implicated synaptic dysfunction in PD pathogenesis. However, how synaptic dysfunction contributes to the vulnerability of human dopaminergic neurons has not been previously explored. Here, we demonstrate that commonly mutated, PD-linked leucine-rich repeat kinase 2 (LRRK2) mediates the phosphorylation of auxilin in its clathrin-binding domain at Ser627. Kinase activity-dependent LRRK2 phosphorylation of auxilin led to differential clathrin binding, resulting in disrupted synaptic vesicle endocytosis and decreased synaptic vesicle density in LRRK2 patient-derived dopaminergic neurons. Moreover, impaired synaptic vesicle endocytosis contributed to the accumulation of oxidized dopamine that in turn mediated pathogenic effects such as decreased glucocerebrosidase activity and increased α-synuclein in mutant LRRK2 neurons. Importantly, these pathogenic phenotypes were partially attenuated by restoring auxilin function in mutant LRRK2 dopaminergic neurons. Together, this work suggests that mutant LRRK2 disrupts synaptic vesicle endocytosis, leading to altered dopamine metabolism and dopamine-mediated toxic effects in patient-derived dopaminergic neurons.

Parkinson's disease | LRRK2 | auxilin | synaptic vesicle endocytosis | DA oxidation

In-depth investigation of genes linked to Parkinson's disease (PD) provides valuable mechanistic insight into pathogenesis for therapeutic development. In particular, recently identified mutations in *DNAJC6* (auxilin) and *SYNJ-1* (synaptojanin 1) in patients with juvenile and early-onset atypical parkinsonism suggest synaptic dysfunction in PD pathogenesis because both genes are involved in clathrin-dependent synaptic vesicle endocytosis (SVE), which replenishes synaptic vesicles following neuronal activity (1–5). Moreover, leucine-rich repeat kinase 2 (LRRK2), the most commonly mutated protein in familial and sporadic PD, has also been implicated in synaptic function (6–9). Pathogenic PD-linked mutations in LRRK2—R1441C/H/G and G2019S—perturb its kinase activity, which is important for SVE and neurotransmission (6, 7, 10), and several SVE proteins, including synaptojanin 1 and endophilin A1, are LRRK2 substrates (11, 12), suggesting that LRRK2 globally regulates SVE via its kinase activity.

Synaptic vesicle pools can be regenerated at the axon terminal through clathrin-mediated SVE, a process tightly controlled by phosphoregulated proteins (13). This pathway initiates when clathrin is recruited to the plasma membrane via adaptor protein 2 (AP-2). A new clathrin-coated vesicle then invaginates from the plasma membrane through the concerted effort of endophilin A1 and synaptojanin 1 and is subsequently cleaved off by dynamin 1. After fission, auxilin binds and recruits hsc70 to remove the clathrin lattice, thereby producing a synaptic vesicle that can be packaged with neurotransmitters. Importantly, loss of individual SVE proteins leads to similar synaptic defects, including increased retention of clathrin-coated vesicles and decreased synaptic vesicle density (14–17). Defective SVE in substantia nigra pars compacta dopaminergic neurons could ultimately

lead to increased cytosolic dopamine (DA) due to inefficient DA packaging, which can be rapidly oxidized to drive downstream toxic effects and subsequent nigrostriatal neurodegeneration (18–23).

However, the connection between synaptic dysfunction and DA-mediated toxic effects has not been previously examined in patient-derived dopaminergic neurons. In this study, we demonstrate that LRRK2 and auxilin interact and that LRRK2 kinase activity mediates auxilin phosphorylation in its clathrin-binding domain at Ser627 to regulate auxilin's binding to clathrin during SVE, suggesting that LRRK2 and auxilin functionally converge on synaptic regulation in PD-affected dopaminergic neurons.

Results

Because LRRK2 cofractionates with the presynaptic protein synapsin and phosphorylates several SVE proteins (11, 12, 24), we hypothesized that LRRK2 might have important kinase function at the synapse and that PD-linked mutations which alter kinase activity would affect synaptic integrity. We generated induced pluripotent stem cell (iPSC)-derived midbrain dopaminergic neurons (*SI Appendix*, Fig. S1) from reprogrammed PD patient fibroblasts harboring the R1441C/G or G2019S mutations, along with healthy control cell lines (*SI Appendix*, Fig. S2) (25, 26). Synaptic proteins primarily involved in SVE, such as auxilin, dynamin 1, AP-2, and endophilin A1, were significantly decreased in LRRK2 R1441G dopaminergic neurons compared with healthy controls (Fig. 1 A–F), while presynaptic marker synaptophysin and β-actin levels remained unaltered. Furthermore,

Significance

Identifying dysfunctional cellular mechanisms in sporadic neurodegenerative diseases has been challenging. Therefore, in-depth investigation of genetic forms of disease can provide valuable insight into pathogenic disease mechanisms. Here, we demonstrate the novel interaction between two Parkinson's disease-linked genes, LRRK2 and auxilin. Additionally, as both genes have described roles at the synapse, we identify synaptic dysfunction as a contributor of dopamine-mediated toxic effects in human dopaminergic neurons. Together, these results highlight the importance of the mechanistic dissection of genetic forms of Parkinson's disease to identify converging pathways and targets for therapeutic intervention.

using a well-established FM 1-43 styryl dye-based endocytic capacity assay, we found that activity-dependent endocytosis was decreased in LRRK2 R1441C/G dopaminergic neurons (Fig. 1 *G* and *H*). Of the proteins decreased in mutant LRRK2 neurons, auxilin has been linked to PD via recently identified mutations (1–3). Auxilin regulates clathrin uncoating by recruiting the ATPase hsc70 to clathrin-coated vesicles and is highly homologous to cyclin-G-associated kinase (*GAK*) (27–29), a PD risk gene which interacts with LRRK2 (30, 31). To determine whether LRRK2 specifically interacts with auxilin, we generated V5-tagged wild-type auxilin and found that auxilin coimmunoprecipitated endogenous LRRK2, as well as hsc70 (Fig. 2*A*). Together, these results suggest that LRRK2 interacts with auxilin to potentially regulate synaptic function.

The LRRK2 G2019S mutation leads to an increase in kinase activity, while the R1441C/H/G mutation has been shown to alter LRRK2 kinase activity by decreasing GDP/GTP cycling, which is essential for kinase activity (10, 32, 33). Additionally, compared with wild-type LRRK2, both mutations have been shown to differentially modulate several SVE phosphosubstrates acting upstream of auxilin (11, 12). Auxilin is a phosphoregulated protein containing numerous serine and threonine residues in both its PTEN-like and clathrin-binding domains. To identify potential LRRK2-mediated auxilin phosphorylation sites, we subjected purified wild-type auxilin to tandem mass spectrometry-based proteomic analysis. FLAG-tagged wild-type auxilin was coexpressed with either wild-type LRRK2, LRRK2 G2019S, LRRK2 R1441C, or EGFP, and auxilin was immunoprecipitated using a FLAG antibody (*SI Appendix*, Fig. S3*A*). From this analysis, we identified auxilin with an amino acid sequence coverage generally >90% and identified an auxilin phosphorylation site at Ser627 located within its clathrin-binding domain in each experimental condition (Fig. 2 *B* and *C*). We additionally performed phosphoanalysis of FLAG-tagged wild-type auxilin purified from cells which were untreated or pretreated with DMSO or the LRRK2 kinase inhibitor GSK2578215A, which attenuated endogenous wild-type LRRK2 kinase activity (*SI Appendix*, Fig. S3 *B–D*) (34). We again identified the same Ser627 phosphosite in untreated and DMSO conditions, but not when the cells were treated with the LRRK2 kinase inhibitor GSK2578215A, suggesting that phosphorylation of auxilin at Ser627 is lost when LRRK2 kinase activity is abolished (*SI Appendix*, Fig. S3 *C* and *D*). Importantly, this phosphosite is localized in auxilin's clathrin-binding domain near a previously identified clathrin-binding motif (Fig. 2*B*) (35), suggesting that Ser627 phosphorylation may have important consequences for auxilin's synaptic function during clathrin-mediated SVE. We also identified two other auxilin phosphosites at Ser49 and Ser59 in proximity to its PTEN-like domain under wild-type LRRK2 and LRRK2 R1441C conditions, but not under the LRRK2 G2019S condition (*SI Appendix*, Fig. S4*A*).

Previous studies have shown that truncated auxilin containing only the clathrin-binding and J domains is sufficient for retaining auxilin function (36, 37). Thus, to determine whether LRRK2 phosphorylation might modulate auxilin's clathrin-binding activity, we further examined the Ser627 phosphorylation site. To first confirm Ser627 as an LRRK2-mediated phosphosite, we generated phosphodeficient auxilin S627A and immunoprecipitated V5-tagged wild-type auxilin or auxilin S627A, as well as wild-type LRRK2 or kinase-dead mutant LRRK2 K1906M, from HEK 293 cells and subjected the purified proteins to in vitro phosphorylation assays. Importantly, wild-type LRRK2, but not kinase-dead LRRK2 K1906M, was sufficient to increase wild-type auxilin's phosphoserine signal (*SI Appendix*, Fig. S3 *E* and *F*). In contrast, the phosphoserine signal for phosphodeficient auxilin S627A was unaltered by either wild-type LRRK2 or kinase-dead LRRK2 K1906M. As an additional control, we confirmed that the phosphoserine signal of wild-type LRRK2, but not that of kinase-dead LRRK2 K1906M, was increased by ATP addition, as expected, since LRRK2 also autophosphorylates itself (*SI Appendix*, Fig. S3*E*) (10). We performed similar in vitro phosphorylation assays using mutant LRRK2 R1441C and found that it increased auxilin phosphorylation state compared with wild-type LRRK2, but importantly, expression of phosphodeficient auxilin S627A decreased auxilin phosphorylation state in the mutant LRRK2 R1441C condition (Fig. 2 *D* and *E*), further suggesting that S627 plays a role in LRRK2-mediated phosphorylation of auxilin. Together, these data suggest that auxilin Ser627 is specifically targeted by LRRK2 kinase activity.

To determine whether auxilin Ser627 phosphorylation regulated its binding to clathrin, we examined the ability of phosphodeficient auxilin S627A and phosphomimetic auxilin S627D to bind clathrin and hsc70. We found that phosphodeficient auxilin S627A coimmunoprecipitated significantly more endogenous clathrin than either wild-type auxilin or phosphomimetic auxilin S627D (Fig. 2 *F* and *G*), while both phosphomutants did not differentially bind hsc70 (Fig. 2 *F* and *H*). To further examine whether de novo LRRK2-mediated phosphorylation of auxilin
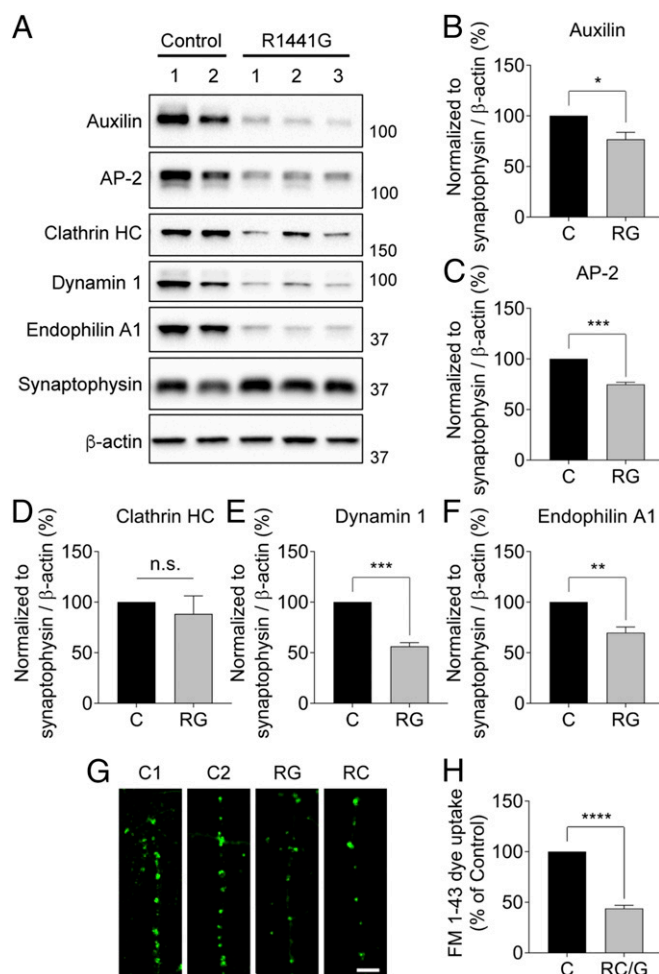

Fig. 1. Dopaminergic neurons from patients with LRRK2-linked PD exhibit decreased levels of SVE proteins. (*A*) Western blot analysis of day 70 dopaminergic neurons probed with auxilin, AP-2, clathrin heavy chain (Clathrin HC), dynamin 1, and endophilin A1. Synaptophysin and β-actin were used as loading controls. (*B–F*) Quantification of Western blots in *A*, normalized to both synaptophysin and β-actin protein signals. (*G*) Representative images of FM 1-43 labeling in human dopaminergic neurons at day 120. (Scale bar: 5 μm.) (*H*) Quantification of FM 1-43 intensity per length of neurite. All data from control lines (C), and similar LRRK2 R1441G (RG) or R1441C (RC) clones were grouped preceding statistical analysis. The results were analyzed using unpaired *t* test (**P* < 0.05, ***P* > 0.005, ****P* < 0.0005, *****P* < 0.00005), with all error bars representing SEM; *n* = 3; n.s., not significant.
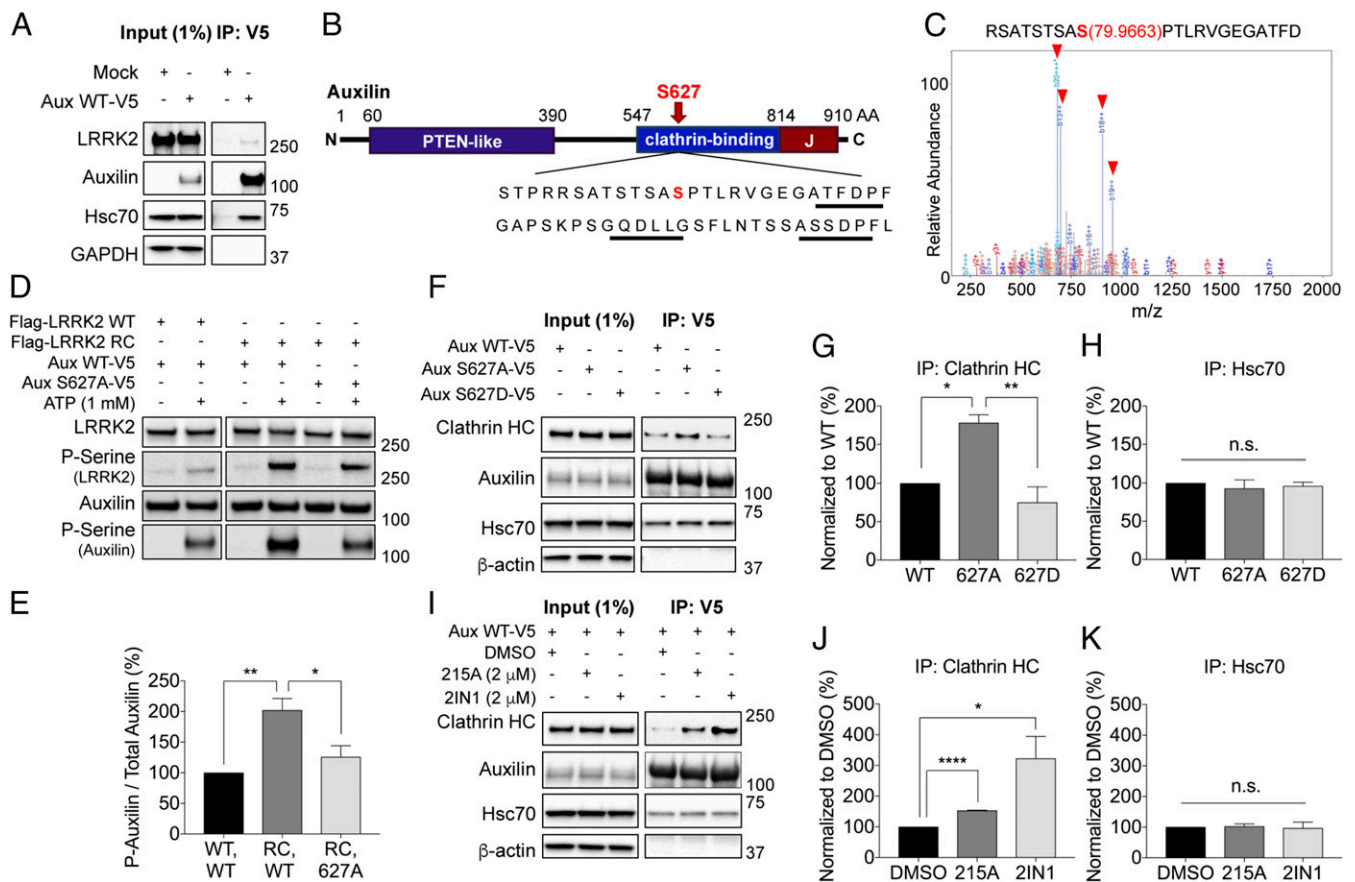
Fig. 2. LRRK2 phosphorylates auxilin in its clathrin-binding domain at Ser627. (*A*) Western blot analysis of coimmunoprecipitated proteins with V5-tagged wild-type auxilin (Aux WT-V5) from HEK 293 cells, probed for LRRK2, auxilin, hsc70 (positive control), and GAPDH (loading control). *Left* blots represent 1% input of whole cell lysate. (*B*) Schematic of auxilin protein mapping the Ser627 phosphosite to its clathrin-binding domain (clathrin-binding motifs are underlined). (*C*) Representative tandem mass spectra identifying phosphorylated Ser627 site in auxilin. B ions containing the phosphate group are indicated (red triangles) [overexpression, $n = 2$; the LRRK2 kinase inhibitor GSK2578215A (2 μM), $n = 1$]. (*D*) Western blot analysis of purified FLAG-tagged LRRK2 WT or LRRK2 R1441C (RC) and of V5-tagged auxilin WT or phosphodeficient auxilin S627A from HEK 293 cells following in vitro phosphorylation assays with or without 1 mM ATP probed for LRRK2, auxilin, and pan-phosphoserine (P-Serine). All experimental conditions were run on the same Western blot. (*E*) Quantification of pan-phosphoserine auxilin (P-Auxilin) signal in *D* normalized to total auxilin levels. (*F*) Western blot analysis of coimmunoprecipitated proteins with V5-tagged auxilin WT and auxilin S627A and S627D from HEK 293 cells probed for clathrin heavy chain (Clathrin HC), auxilin, hsc70, and β-actin (loading control). *Left* blots represent 1% input of whole cell lysate. (*G* and *H*) Quantification of coimmunoprecipitated clathrin and hsc70 normalized to immunoprecipitated auxilin in *F*. (*I*) Western blot analysis of coimmunoprecipitated proteins with V5-tagged auxilin WT upon LRRK2 kinase inhibitor [GSK2578215A (215A, 2 μM) or LRRK2-IN-1 (2IN1, 2 μM)] treatment in HEK 293 cells probed for clathrin HC, auxilin, hsc70, and β-actin. *Left* blots represent 1% input of whole cell lysate. (*J* and *K*) Quantification of coimmunoprecipitated clathrin and hsc70 normalized to immunoprecipitated auxilin in *I*. All results were analyzed using one-way ANOVA statistical analysis (*$P < 0.05$, **$P < 0.005$, ****$P < 0.00005$), with all error bars representing SEM; $n = 3$. IP, immunoprecipitation; n.s., not significant.

could affect its function, we overexpressed V5-tagged wild-type auxilin in HEK 293 cells and treated cells with either DMSO or an LRRK2 kinase inhibitor (GSK2578215A or LRRK2-IN-1). Upon inhibiting LRRK2 kinase activity, auxilin binding to clathrin was significantly increased (Fig. 2 *I* and *J* and *SI Appendix*, Fig. S3 *G* and *H*), consistent with our observations of increased clathrin-binding by phosphodeficient auxilin S627A (Fig. 2 *F* and *G*), whereas auxilin binding to hsc70 was not altered, as expected (Fig. 2 *I* and *K*). To determine whether additional auxilin phosphosites (Ser49 and Ser59) identified through mass spectrometry analysis also regulated auxilin's clathrin-binding function, we overexpressed phosphodeficient auxilin S49A and S59A and phosphomimetic auxilin S49D and S59D in HEK 293 cells and coimmunoprecipitated clathrin and hsc70. Both phosphodeficient S49A and S59A did not bind more clathrin or hsc70 as compared with wild-type auxilin (*SI Appendix*, Fig. S4 *B–G*). Taken together, these data suggest that LRRK2-mediated phosphorylation of auxilin in the clathrin-binding domain at Ser627 preferentially alters its ability to bind clathrin during SVE.

To further determine whether altered synaptic protein function might disrupt synaptic vesicle density and morphology in LRRK2 PD patient neurons, we analyzed iPSC-derived dopaminergic neurons by transmission electron microscopy (TEM). LRRK2 R1441C dopaminergic neurons showed significantly reduced synaptic vesicle densities by ~40% compared with healthy control neurons (Fig. 3 *A* and *C*) and contained synaptic vesicles lacking distinct surrounding membranes, consistent with membraneless clathrin cages observed in auxilin knockout mice due to loss of auxilin function and defective clathrin uncoating (Fig. 3*A*, highlighted in enlarged *Insets* of LRRK2 R1441C synapse) (14). Membraneless clathrin cages in mutant LRRK2 neurons did not result from improper fixation, as synaptic plasma membranes were still clearly observed in these neurons. Enlarged endosomal-like vacuoles were also observed in the presynaptic terminal of LRRK2 R1441C neurons, indicative of defective SVE (38, 39) (Fig. 3 *B* and *D*).

Efficient packaging of DA into synaptic vesicles is dependent on properly regenerated synaptic vesicles at the presynaptic terminal (40). Because we observed decreased synaptic vesicles
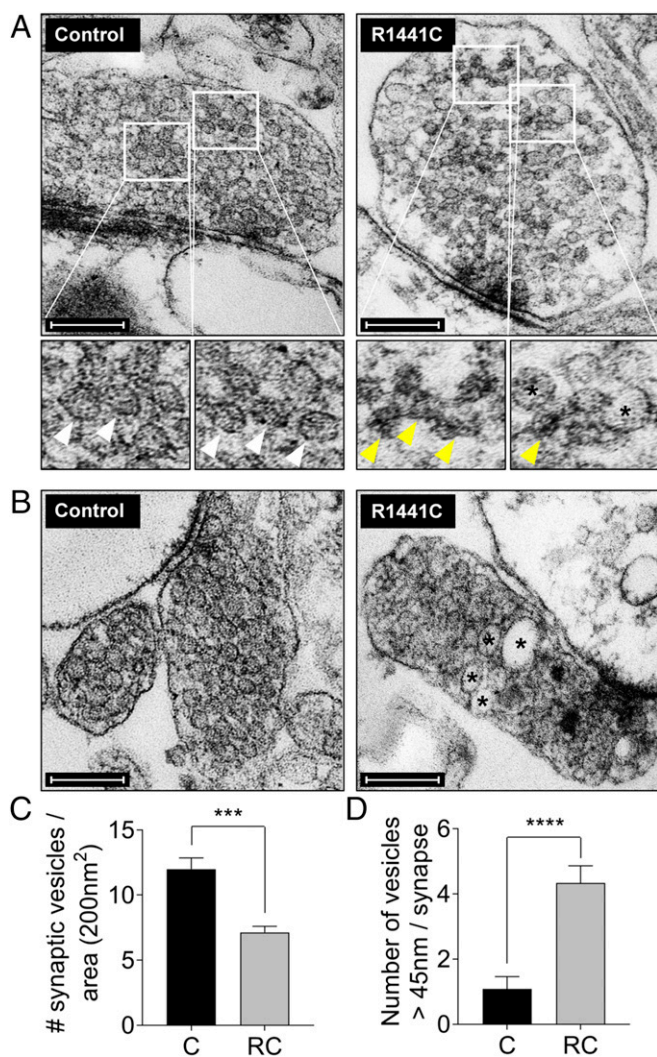
Fig. 3. Synaptic abnormalities in mutant LRRK2 dopaminergic neurons. (*A*) TEM analysis of human dopaminergic neurons at day 100. (Scale bar: 200 nm.) *Bottom* panels display higher magnification of *Insets* in *Top* to show the presence of membraneless clathrin cages and enlarged endosomal-like (black asterisks) vacuoles in mutant neurons. (*Insets*) Synaptic vesicles are identified with white arrowheads (control), and membraneless clathrin cages are indicated with yellow arrowheads (mutant). (*B*) TEM analysis of enlarged endosomal-like vacuoles (black asterisks) in dopaminergic neurons. (*C*) Quantification of synaptic vesicle density in *A*. (*D*) Quantification of the number of enlarged synaptic compartments per synapse in *B*. All comparisons were made between control (C) and LRRK2 R1441C (RC) dopaminergic neurons, and results were analyzed using an unpaired *t* test (***P < 0.0005, ****P > 0.00005), with error bars representing SEM; *n* = 10 and 12 images, respectively.

in mutant LRRK2 neurons, we hypothesized that defective SVE might lead to elevated cytosolic DA levels, which can be further oxidized to generate DA-quinones and aminochromes (18, 19). We found that oxidized DA levels were significantly increased in LRRK2 R1441C/G and G2019S dopaminergic neurons compared with healthy control neurons in a time-dependent manner (Fig. 4 *A*–*C* and *SI Appendix*, Fig. S5 *A* and *B*). However, tyrosine hydroxylase levels were unaltered, demonstrating that increased oxidized DA was not due to increased DA synthesis (*SI Appendix*, Fig. S6). Our previous work showed that increased oxidized DA modifies lysosomal glucocerebrosidase (GCase), leading to decreased activity (41), and that increased α-synuclein (α-Syn) levels correlate with decreased GCase activity (26). Here, we found that LRRK2 R1441C/G and G2019S dopaminergic neurons

displayed decreased GCase activity and increased α-Syn levels compared with healthy control neurons (Fig. 4 *D*–*F* and *SI Appendix*, Fig. S5 *C*–*E*).

Lastly, to examine whether increased oxidized DA in mutant LRRK2 dopaminergic neurons was due to auxilin dysfunction, we transduced healthy control and mutant LRRK2 R1441G dopaminergic neurons with wild-type auxilin at day 70 post-differentiation and analyzed the oxidized DA levels at day 100. Importantly, increased expression of wild-type auxilin led to (*i*) significantly decreased oxidized DA in mutant LRRK2 R1441G neurons (Fig. 4 *G* and *H* and *SI Appendix*, Fig. S7 *A* and *B*), (*ii*) further reduced α-Syn levels, and (*iii*) significantly increased GCase activity (Fig. 4 *I*–*K*). Moreover, levels of synaptic proteins involved in SVE, such as AP-2, clathrin, dynamin 1, and endophilin A1, remained reduced, further suggesting that accumulation of oxidized DA in LRRK2 mutant neurons is attenuated by directly restoring auxilin function in SVE (*SI Appendix*, Fig. S7).

Discussion

In this study, we showed that auxilin and LRRK2 interact and that LRRK2-mediated phosphorylation of auxilin at Ser627, located within its clathrin-binding domain, leads to differential association of auxilin with clathrin and disrupts SVE, resulting in decreased synaptic vesicle density in mutant LRRK2 dopaminergic neuron synapses. Consequently, disrupted SVE contributes to the accumulation of oxidized DA and its downstream effects, including increased α-Syn and decreased GCase activity, which were all attenuated by restoring auxilin function.

LRRK2 has been shown to interact with and phosphoregulate several SVE proteins, including endophilin A1 and synaptojanin, both of which have distinct roles upstream of auxilin (13). Moreover, LRRK2 G2019S-mediated phosphorylation of endophilin A1 alters its ability to associate with membranes, while LRRK2 R1441C knockin *Drosophila* models displayed an altered presynaptic proteome and LRRK2-mediated phosphorylation of synaptojanin 1 (11, 12), suggesting that LRRK2 has an important regulatory kinase role for multiple proteins at the presynaptic terminal. Interestingly, mutations in *SYNJ-1* (synaptojanin 1) also lead to early-onset atypical parkinsonism (4, 5), and the loss of either endophilin A1 or synaptojanin 1 in knockout mouse models results in defective SVE (16, 17). In line with this, we found that dopaminergic neurons derived from LRRK2 R1441G patients had decreased levels of SVE proteins (including auxilin, AP-2, endophilin A1, synaptojanin 1, and dynamin 1) as well as decreased activity-dependent endocytic capacity, indicative of defective SVE.

Interestingly, LRRK2 has also been shown to interact in complex with GAK (30), a ubiquitously expressed clathrin uncoating protein localized at the trans-Golgi network (42). GAK is highly homologous to auxilin and is also a PD risk factor (29, 31). Here, we show that LRRK2 and auxilin also interact. Through tandem mass spectrometry, we determined that wild-type LRRK2 and the PD-linked LRRK2 mutants R1441C and G2019S phosphorylate auxilin at Ser627 and that this phosphorylation was abolished by the LRRK2 kinase inhibitor GSK2578215A. Generation of a phosphodeficient auxilin S627A resulted in a significantly reduced auxilin phosphorylation state in the presence of wild-type LRRK2, LRRK2 R1441C, or kinase-dead LRRK2 K1906M. As the Ser627 phosphosite is located within auxilin's clathrin-binding domain, which is important for recognizing and binding to clathrin-coated vesicles (35), we further found that inhibition of endogenous LRRK2 kinase activity or expression of phosphodeficient auxilin S627A, but not phosphomimetic auxilin S627D, resulted in increased auxilin association with clathrin. These data thus further validate auxilin Ser627 as an LRRK2 kinase activity-dependent phosphosite that is important in modulating auxilin binding to clathrin.

Using TEM, we also observed decreased synaptic vesicle density in presynaptic terminals of LRRK2 R1441C dopaminergic neurons, indicative of defective SVE. These data are consistent with studies
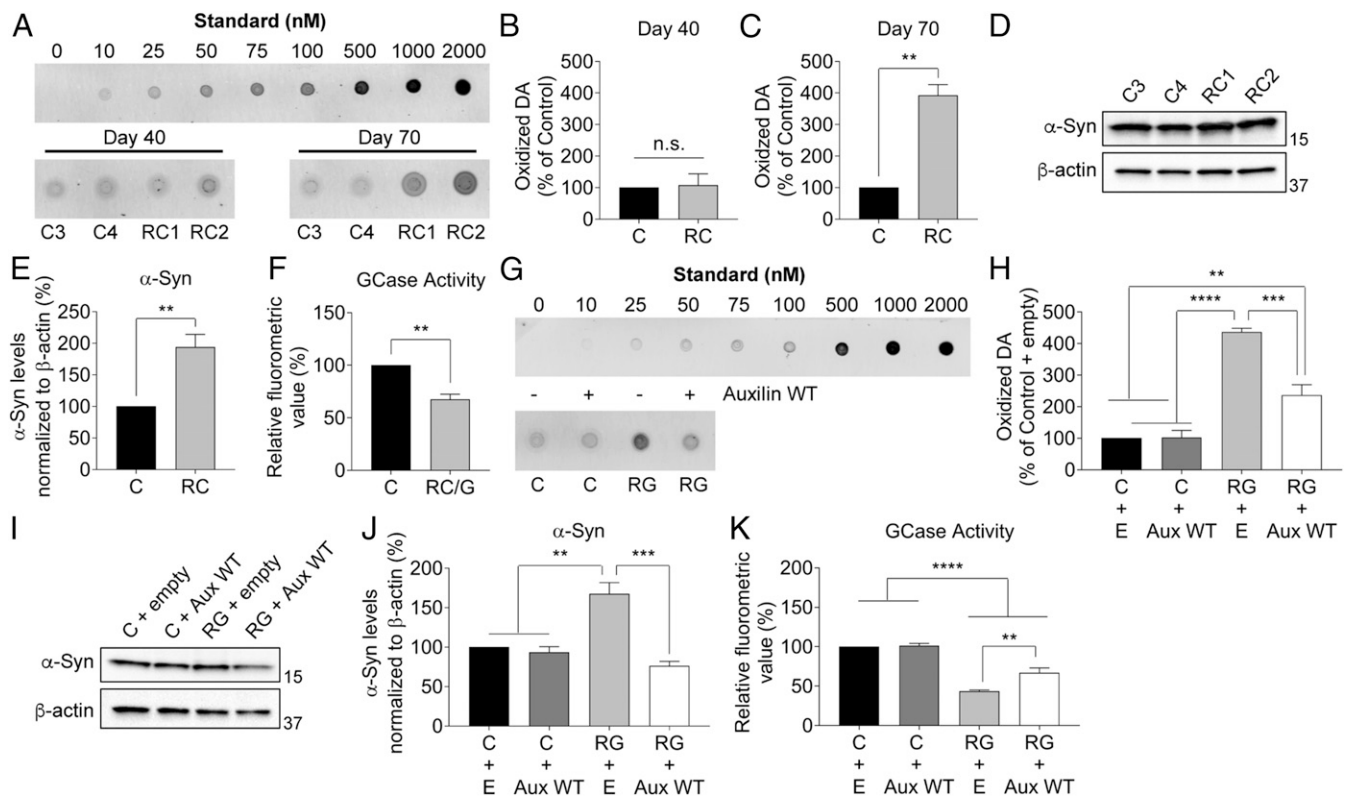
Fig. 4. Expression of wild-type auxilin partially rescues pathogenic phenotypes in mutant LRRK2 dopaminergic neurons. (*A*) Near-IR fluorescence analysis of human dopaminergic neurons at day 40 and 70. (*B* and *C*) Quantification of oxidized DA levels in dopaminergic neurons at day 40 and 70, respectively. (*D*) Western blot analysis of human dopaminergic neurons at day 100. The blot was probed with α-Syn and β-actin antibodies. (*E*) Quantification of *D*. (*F*) GCase activity in whole cell lysate of human dopaminergic neurons at day 100. (*G*) Near-IR fluorescence analysis of human dopaminergic neurons at day 100 following transduction of either empty vector (E) or wild-type (WT) auxilin for 30 d, starting at day 70 postdifferentiation. (*H*) Quantification of oxidized DA levels in *G*. (*I*) Western blot analysis of dopaminergic neurons following transduction with auxilin WT at day 100. The blot was probed with α-Syn and β-actin antibodies. (*J*) Quantification of *I*. (*K*) GCase activity in whole cell lysate of transduced auxilin WT dopaminergic neurons at day 100. All data from control (C) lines, and similar LRRK2 R1441C (RC) or R1441G (RG) mutations were grouped preceding statistical analysis. The results were analyzed using unpaired *t* test or one-way ANOVA (**$P < 0.005$, ***$P < 0.0005$, ****$P < 0.00005$), with all error bars representing SEM; $n = 3$; n.s., not significant.

of knockout mouse models for endophilin A1, synaptojanin 1, dynamin 1, or auxilin (14–17). Auxilin knockout mouse models also display an increased presence of membraneless clathrin cages, a unique structural feature that results from delays in SVE due to auxilin loss of function (14). We observed a similar structural feature in LRRK2 R1441C dopaminergic nerve terminals, suggesting that synaptic defects in mutant LRRK2 neurons are mediated through auxilin loss of function. In addition to this, several studies have found that delays in SVE result in enlarged endosomal-like structures, which we similarly observed in LRRK2 R1441C dopaminergic neurons (38, 39), providing further support that SVE is impaired by PD-linked mutations in LRRK2.

Our recent data showed that DA plays an important role in dysfunction and degeneration of midbrain dopaminergic neurons (41). In the nerve terminal, DA is rapidly packaged into an incoming population of regenerated synaptic vesicles. Efficient vesicular function and storage of DA is critical for maintaining low levels of cytosolic DA (20–23). Because cytosolic DA can be rapidly oxidized (18, 19), we observed increased levels of oxidized DA in LRRK2 R1441C/G and G2019S dopaminergic neurons, indicative of increased cytosolic DA levels. We also previously showed that increased oxidized DA can modulate GCase at a cysteine residue within its active domain and that increased α-Syn levels correlate with decreased GCase activity (26, 41). Consistent with this, we also found decreased GCase activity and increased α-Syn levels in mutant LRRK2 dopaminergic neurons. Importantly, by expressing wild-type auxilin, the

levels of oxidized DA could be reduced and downstream DA-mediated effects attenuated, highlighting the importance of mutant LRRK2-mediated auxilin dysfunction in the generation of toxic oxidized DA following defective SVE.

In conclusion, we find that LRRK2 kinase activity regulates the phosphorylation state of auxilin, an important mediator of SVE linked to juvenile and early-onset forms of atypical parkinsonism (1–3), resulting in disrupted SVE in LRRK2 patient-derived dopaminergic neurons. Moreover, these defects in synaptic function may further contribute to DA-mediated toxicity and ultimately drive dopaminergic neurodegeneration in LRRK2-linked PD.

Materials and Methods

Detailed materials and methods are included in *SI Appendix, Materials and Methods*. Reprogrammed iPSCs were differentiated as previously described (25, 26). Before differentiation, iPSCs were treated with Accutase cell detachment solution and seeded onto six-well plates at a density of 1 million cells per well. iPSCs were continuously fed until 80% confluency and differentiation protocols were initiated (day 0). Cells were fed a combination of LDN193189, SB431542, sonic hedgehog, purmorphamine, FGF8, and CHIR99021. On day 13, cells were transferred to poly-D-lysine/laminin–coated 10-cm plates. Cells were fed every third day by half volume feeding with Neurobasal + SM1 supplement and BDNF, ascorbic acid, glial cell line-derived neurotrophic factor, TGF-β3, cAMP, and DAPT until day 40. On day 25, cells were finally passaged onto poly-D-lysine/laminin–coated tissue culture plates. Neurons were continuously fed by half volume feeding every third or fourth day with Neurobasal + SM1 supplement until indicated time points (day 40+).

1. Edvardson S, et al. (2012) A deleterious mutation in *DNAJC6* encoding the neuronal-specific clathrin-uncoating co-chaperone auxilin, is associated with juvenile parkinsonism. *PLoS One* 7:e36458.
2. Köroğlu Ç, Baysal L, Cetinkaya M, Karasoy H, Tolun A (2013) DNAJC6 is responsible for juvenile parkinsonism with phenotypic variability. *Parkinsonism Relat Disord* 19:320–324.
3. Olgiati S, et al.; International Parkinsonism Genetics Network (2016) *DNAJC6* mutations associated with early-onset Parkinson's disease. *Ann Neurol* 79:244–256.
4. Quadri M, et al.; International Parkinsonism Genetics Network (2013) Mutation in the *SYNJ1* gene associated with autosomal recessive, early-onset Parkinsonism. *Hum Mutat* 34:1208–1215.
5. Olgiati S, et al. (2014) PARK20 caused by *SYNJ1* homozygous Arg258Gln mutation in a new Italian family. *Neurogenetics* 15:183–188.
6. Di Fonzo A, et al.; Italian Parkinson Genetics Network (2005) A frequent LRRK2 gene mutation associated with autosomal dominant Parkinson's disease. *Lancet* 365:412–415.
7. Gilks WP, et al. (2005) A common LRRK2 mutation in idiopathic Parkinson's disease. *Lancet* 365:415–416.
8. Arranz AM, et al. (2015) LRRK2 functions in synaptic vesicle endocytosis through a kinase-dependent mechanism. *J Cell Sci* 128:541–552.
9. Shin N, et al. (2008) LRRK2 regulates synaptic vesicle endocytosis. *Exp Cell Res* 314:2055–2065.
10. Webber PJ, et al. (2011) Autophosphorylation in the leucine-rich repeat kinase 2 (LRRK2) GTPase domain modifies kinase and GTP-binding activities. *J Mol Biol* 412:94–110.
11. Matta S, et al. (2012) LRRK2 controls an EndoA phosphorylation cycle in synaptic endocytosis. *Neuron* 75:1008–1021.
12. Islam MS, et al. (2016) Human R1441C LRRK2 regulates the synaptic vesicle proteome and phosphoproteome in a *Drosophila* model of Parkinson's disease. *Hum Mol Genet* 25:5365–5382.
13. Cousin MA, Robinson PJ (2001) The dephosphins: Dephosphorylation by calcineurin triggers synaptic vesicle endocytosis. *Trends Neurosci* 24:659–665.
14. Yim YI, et al. (2010) Endocytosis and clathrin-uncoating defects at synapses of auxilin knockout mice. *Proc Natl Acad Sci USA* 107:4412–4417.
15. Ferguson SM, et al. (2007) A selective activity-dependent requirement for dynamin 1 in synaptic vesicle endocytosis. *Science* 316:570–574.
16. Milosevic I, et al. (2011) Recruitment of endophilin to clathrin-coated pit necks is required for efficient vesicle uncoating after fission. *Neuron* 72:587–601.
17. Kim WT, et al. (2002) Delayed reentry of recycling vesicles into the fusion-competent synaptic vesicle pool in synaptojanin 1 knockout mice. *Proc Natl Acad Sci USA* 99:17143–17148.
18. Graham DG (1978) Oxidative pathways for catecholamines in the genesis of neuromelanin and cytotoxic quinones. *Mol Pharmacol* 14:633–643.
19. Hastings TG, Lewis DA, Zigmond MJ (1996) Role of oxidation in the neurotoxic effects of intrastriatal dopamine injections. *Proc Natl Acad Sci USA* 93:1956–1961.
20. Lohr KM, et al. (2014) Increased vesicular monoamine transporter enhances dopamine release and opposes Parkinson disease-related neurodegeneration in vivo. *Proc Natl Acad Sci USA* 111:9977–9982.
21. Dunn AR, et al. (2017) Synaptic vesicle glycoprotein 2C (SV2C) modulates dopamine release and is disrupted in Parkinson disease. *Proc Natl Acad Sci USA* 114:E2253–E2262.
22. Caudle WM, et al. (2007) Reduced vesicular storage of dopamine causes progressive nigrostriatal neurodegeneration. *J Neurosci* 27:8138–8148.
23. Vergo S, Johansen JL, Leist M, Lotharius J (2007) Vesicular monoamine transporter 2 regulates the sensitivity of rat dopaminergic neurons to disturbed cytosolic dopamine levels. *Brain Res* 1185:18–32.
24. Biskup S, et al. (2006) Localization of LRRK2 to membranous and vesicular structures in mammalian brain. *Ann Neurol* 60:557–569.
25. Kriks S, et al. (2011) Dopamine neurons derived from human ES cells efficiently engraft in animal models of Parkinson's disease. *Nature* 480:547–551.
26. Mazzulli JR, et al. (2011) Gaucher disease glucocerebrosidase and α-synuclein form a bidirectional pathogenic loop in synucleinopathies. *Cell* 146:37–52.
27. Eisenberg E, Greene LE (2007) Multiple roles of auxilin and hsc70 in clathrin-mediated endocytosis. *Traffic* 8:640–646.
28. Morgan JR, Prasad K, Jin S, Augustine GJ, Lafer EM (2001) Uncoating of clathrin-coated vesicles in presynaptic terminals: Roles for Hsc70 and auxilin. *Neuron* 32:289–300.
29. Lemmon SK (2001) Clathrin uncoating: Auxilin comes to life. *Curr Biol* 11:R49–R52.
30. Beilina A, et al.; International Parkinson's Disease Genomics Consortium; North American Brain Expression Consortium (2014) Unbiased screen for interactors of leucine-rich repeat kinase 2 supports a common pathway for sporadic and familial Parkinson disease. *Proc Natl Acad Sci USA* 111:2626–2631.
31. Nalls MA, et al.; International Parkinson's Disease Genomics Consortium (IPDGC); Parkinson's Study Group (PSG) Parkinson's Research: The Organized GENetics Initiative (PROGENI); 23andMe; GenePD; NeuroGenetics Research Consortium (NGRC); Hussman Institute of Human Genomics (HIHG); Ashkenazi Jewish Dataset Investigator; Cohorts for Health and Aging Research in Genetic Epidemiology (CHARGE); North American Brain Expression Consortium (NABEC); United Kingdom Brain Expression Consortium (UKBEC); Greek Parkinson's Disease Consortium; Alzheimer Genetic Analysis Group (2014) Large-scale meta-analysis of genome-wide association data identifies six new risk loci for Parkinson's disease. *Nat Genet* 46:989–993.
32. West AB, et al. (2007) Parkinson's disease-associated mutations in LRRK2 link enhanced GTP-binding and kinase activities to neuronal toxicity. *Hum Mol Genet* 16:223–232.
33. Lewis PA, et al. (2007) The R1441C mutation of LRRK2 disrupts GTP hydrolysis. *Biochem Biophys Res Commun* 357:668–671.
34. Reith AD, et al. (2012) GSK2578215A; a potent and highly selective 2-arylmethyloxy-5-substitutent-N-arylbenzamide LRRK2 kinase inhibitor. *Bioorg Med Chem Lett* 22:5625–5629.
35. Scheele U, et al. (2003) Molecular and functional characterization of clathrin- and AP-2-binding determinants within a disordered domain of auxilin. *J Biol Chem* 278:25357–25368.
36. Massol RH, Boll W, Griffin AM, Kirchhausen T (2006) A burst of auxilin recruitment determines the onset of clathrin-coated vesicle uncoating. *Proc Natl Acad Sci USA* 103:10265–10270.
37. Ma Y, et al. (2002) Identification of domain required for catalytic activity of auxilin in supporting clathrin uncoating by Hsc70. *J Biol Chem* 277:49267–49274.
38. Jakobsson J, et al. (2008) Role of epsin 1 in synaptic vesicle endocytosis. *Proc Natl Acad Sci USA* 105:6445–6450.
39. Zhang B, et al. (1998) Synaptic vesicle size and number are regulated by a clathrin adaptor protein required for endocytosis. *Neuron* 21:1465–1475.
40. Lotharius J, Brundin P (2002) Pathogenesis of Parkinson's disease: Dopamine, vesicles and alpha-synuclein. *Nat Rev Neurosci* 3:932–942.
41. Burbulla LF, et al. (2017) Dopamine oxidation mediates mitochondrial and lysosomal dysfunction in Parkinson's disease. *Science* 357:1255–1261.
42. Lee DW, Wu X, Eisenberg E, Greene LE (2006) Recruitment dynamics of GAK and auxilin to clathrin-coated pits during endocytosis. *J Cell Sci* 119:3502–3512.

NEUROSCIENCE